Synthesis, photochromic behaviour and light-controlled complexation of 3,3-diphenyl-3*H*-benzo[*f*]chromenes containing a dimethylamino group or an aza-15-crown-5 ether unit

Olga A. Fedorova,*[a] François Maurel,[b] Evgeny N. Ushakov,[c] Valery B. Nazarov,[c] Sergey P. Gromov,[a] Anna V. Chebunkova,[a] Alexei V. Feofanov,[d] Iouri S. Alaverdian,[d] Michael V. Alfimov[a] and Francesco Barigelletti[e]

[a] *Photochemistry Center of Russian Academy of Sciences, Novatorov str, 7a, 117421 Moscow, Russian Federation. E-mail: fedorova@photonics.ru; Fax: 095 936 1255; Tel: 095 936 3850*

[b] *ITODYS, Université Paris 7, CNRS (ESA 7086), 1 Rue Guy de la Brosse, 75005 Paris, France*

[c] *Institute of Problems of Chemical Physics of Russian Academy of Sciences, 142432 Chernogolovka, Moscow Region, Russian Federation*

[d] *Shemyakin-Ovchinnikov Institute of Bioorganic Chemistry, Russian Academy of Sciences, ul. Miklukho-Maklaya 16/10, 117997 Moscow, Russian Federation*

[e] *Instituto FRAE-CNR, Via P. Gobetti 101, 40129 Bologna, Italy*

Received (in Montpellier, France) 30th April 2003, Accepted 4th August 2003
First published as an Advance Article on the web 17th September 2003

Synthesis of 3,3-diphenyl-3*H*-benzo[*f*]chromenes containing an aza-15-crown-5-ether unit or a dimethylamino group and spectrokinetic study of light-controlled complexation of these compounds with Ca^{2+} in acetonitrile are reported. The affinity of the azacrown chromene to Ca^{2+} decreases substantially upon a photoinduced ring-opening reaction. In contrast, dimethylamino chromene, which is unable to bind Ca^{2+} in the dark, shows a low cation-binding capacity upon UV irradiation. The spectroscopic and kinetic behaviour of the photomerocyanine isomers of these chromenes is strongly affected by complexation with Ca^{2+}. A semi-empirical quantum-chemical study of the merocyanine isomers was applied to interpret the experimental data.

Introduction

Crown ethers containing a photoresponsive unit are of current interest because of their potential applications as optical sensors for metal ions and elements of photoswitchable molecular devices.[1] Several reversible photochemical reactions, such as geometric isomerisation of azobenzene[2] and styryl compounds,[3] dimerisation of anthracene,[4] and photochromic reaction of spiro compounds,[5] have been employed to provide photocontrol over a metal ion-binding capacity of crown ethers. Recently, the first representative of crown-containing photochromic chromenes has been reported.[6] In the cited study, the photocontrolled binding of Pb^{2+} by benzo-15-crown-5 ether-containing naphthopyran was studied by electrochemical methods. This chromene was reported to bind Pb^{2+} in the dark, with detachment of Pb^{2+} upon UV irradiation. However, no data on the binding constants or structures of the complexes formed were presented for this system.

The transient merocyanine form of crown-containing chromenes has an additional cation-binding site as compared with the thermodynamically stable closed form, *viz*., carbonyl oxygen. Therefore, the two forms of crown-containing chromenes can differ not only in the cation-binding capacity but also in the composition and/or structure of their metal complexes. In order to estimate the potential of crown-containing chromenes as photoswitchable ionophores, more comprehensive studies of their complexation are needed.

For this purpose, we synthesised novel azacrown-containing 3,3-diphenyl-3*H*-benzo[*f*]chromene **1b** (Scheme 1) and carried out a spectrokinetic study of its light-controlled complexation with Ca^{2+} in acetonitrile. Dimethylamino-substituted 3,3-diphenyl-3*H*-benzo[*f*]chromene **1c** was prepared as a reference compound.[7,8] Combined analysis of the spectroscopic and kinetic data obtained in the absence/presence of Ca^{2+} allowed us to determine the stability constants, the absorption spectra, and the dark lifetimes for Ca^{2+} complexes of the transient photomerocyanine isomers of **1a**,**b**. A quantum-chemical study of the photomerocyanine isomers was carried out in order to verify some conclusions drawn on the basis of the experimental results.

Results and discussion

Synthesis and spectrokinetic studies

The benzochromenes **1a** and **1b** were synthesised according to the three-step procedure represented in Scheme 1. The structures attributed to **1a** and **1b** were confirmed by ^{1}H NMR spectroscopy data.

The addition of $Ca(ClO_4)_2$ did not influence the NMR spectrum of **1a** in a MeCN-d_3 solution. In contrast, the addition of an equimolar amount of $Ca(ClO_4)_2$ to a MeCN-d_3 solution of **1b** led to significant changes in the proton chemical shifts (see Experimental Section). The most pronounced downfield shifts were observed for the signals from the methylene protons of the crown ether fragment ($\Delta\delta$ is up to 0.38, $\Delta\delta = \delta_{complex} - \delta_{ligand}$) and from the protons of the C(1)=C(2) double bond ($\Delta\delta$ is up to 0.12). These shifts indicate the formation of a

 DOI: 10.1039/b304874h

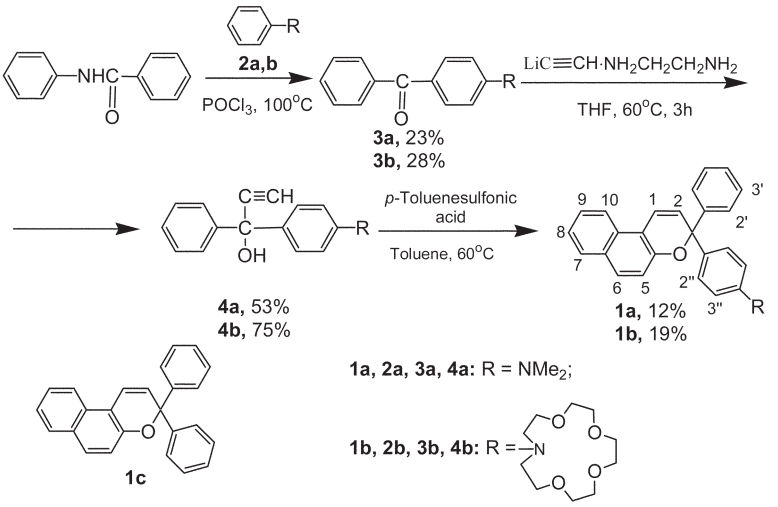

Scheme 1

complex between chromene **1b** and Ca^{2+} through the crown ether fragment (Scheme 2).

The signals from the 2″ and 3″ protons of the phenylazacrown ether moiety of free **1b** are located in a lower field than the signals from the corresponding 2′ and 3′ protons of the unsubstituted benzene ring (Table 1). This is due to the electron-donating effect of the nitrogen atom of the azacrown ether fragment. Upon complexation of **1b** with Ca^{2+}, the magnitudes of the chemical shifts for the corresponding protons of the two phenyl rings in **1b** become very similar. This can be explained by the fact that the coordination of Ca^{2+} to the crown ether ring diminishes the electron-donating effect of the nitrogen atom.

Compounds **1a**,**b** in MeCN exhibited very similar UV/Vis absorption spectra. The main spectroscopic feature distinguishing these compounds from benzochromene **1c** is the presence of an additional absorption band with a maximum around 265 nm. The addition of $Ca(ClO_4)_2$ to a solution of **1b** led to the disappearance of this band, indicating that Ca^{2+} is bound by the macrocyclic unit of **1b**. In contrast, the absorption spectrum of **1a** was not affected even at a high $Ca(ClO_4)_2$ concentration (0.1 mol dm^{-3}).

The spectra of **1b** measured at various concentrations of $Ca(ClO_4)_2$ (Fig. 1) were analysed using a matrix modelling method.[9] This analysis provided evidence for 1 : 1 complexation between **1b** and Ca^{2+} and allowed the corresponding complex stability constant to be estimated (Table 2).

UV irradiation of **1b** in MeCN led to the appearance of a broad absorption band in the visible region, which was assigned to the merocyanine isomer **P1b** (Scheme 3). The dark ring-closure reaction for **P1b** occurred with a rate constant k_d of about 0.6 s^{-1} and resulted in the initial chromene. The photochromic behaviour of compound **1a** was very similar to that of **1b**.

We supposed that the main complexation parameters of transient merocyanine isomers could be determined using a spectrokinetic approach. A high concentration of $Ca(ClO_4)_2$

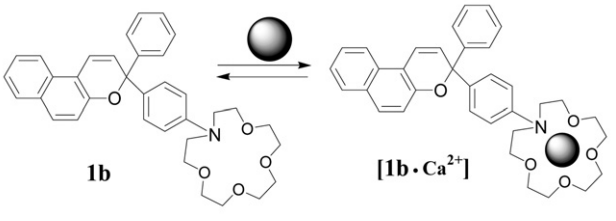

Scheme 2

Table 1 The chemical shifts (δ, ppm) of the phenyl ring protons of free and complexed **1b** in MeCN

Compound	H–C(2′)	H–C(2″)	H–C(3′)	H–C(3″)
1b	7.53	7.26	7.36	6.63
[1b Ca^{2+}]	7.57	7.59	7.38	7.31

led to a significant increase in the dark lifetime of photomerocyanines **P1a** and **P1b** and caused strong shifts in their absorption spectra, indicating that these compounds were able to bind Ca^{2+}. In order to study the complex formation of Ca^{2+} with the photomerocyanines, the absorption spectrum of **P1a** (**P1b**) under a photostationary equilibrium attained on irradiation of **1a** (**1b**) with 365 nm light and the rate constant k_d for **P1a** (**P1b**) were measured as functions of the concentration, C_M, of $Ca(ClO_4)_2$ added. Since the dark ring closure for the Ca^{2+}-complexed form of **P1a** (**P1b**) should be accompanied by Ca^{2+} detachment from merocyanine oxygen, the titration data were analysed assuming that the rate constant for dark ring closure was much lower than the corresponding rate constant for decomplexation. Examination of a wide set of kinetic data on cation–macrocycle interactions[10] showed that this assumption was very reasonable.

The dependences of k_d on C_M were interpreted in terms of complexation models involving one equilibrium for **P1a**

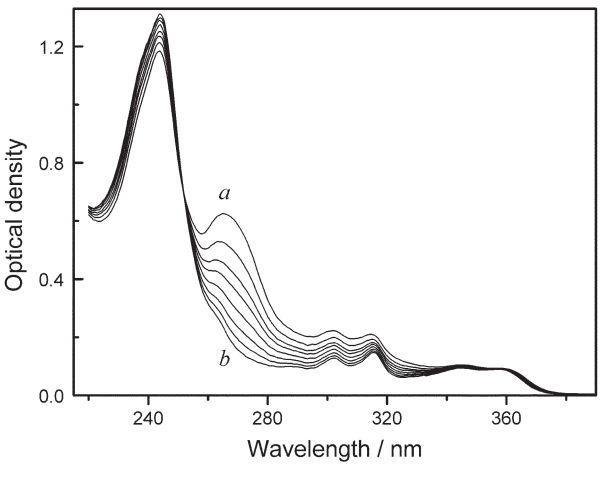

Fig. 1 Absorption spectra of **1b** (2×10^{-5} mol dm^{-3}) in a MeCN solution containing $Ca(ClO_4)_2$ at various concentrations ranging from 0 (*a*) to 5×10^{-4} (*b*) mol dm^{-3}.

Table 2 Stability constants for the complexes of **P1a, 1b** and **P1b** with Ca^{2+}, and spectrokinetic data for **P1a–c**.[a] (Note: order of lines changed to follow order of Table 6)

	log K^b	λ_{max}/nm	k_d/s^{-1}
P1a		538	0.58
[**P1a**·Ca^{2+}]	1.7	672	$\leq$ 0.01
1b·Ca^{2+}	4.9		
P1b		543	0.56
[**P1b**·Ca^{2+}]	4.1	440	0.16
[**P1b**·$(Ca^{2+})_2$]	1.0	507	$\leq$ 0.01
P1c		425	0.11

[a] In acetonitrile at 20 ± 1 °C [b] For [**P1b**·$(Ca^{2+})_2$], K is K_2 of eqn. 2.

(eqn. (1)) and two equilibria for **P1b** (eqns. (1) and (2)):

$$\mathbf{P} + Ca^{2+} \overset{K_1}{\rightleftharpoons} \mathbf{P}Ca^{2+} \quad (1)$$

$$\mathbf{P}Ca^{2+} + Ca^{2+} \overset{K_2}{\rightleftharpoons} \mathbf{P}(Ca^{2+})_2 \quad (2)$$

where **P** is the photomerocyanine, K_1 and K_2 are the stability constants of complexes. The values of K_1 and K_2 were derived using the procedure of non-linear fitting of the kinetic data (Fig. 2) to eqn. (3) for **P1a** or to eqn. (4) for **P1b**:

$$k_d = \frac{k_{d1} + k_{d2}K_1C_M}{1 + K_1C_M} \quad (3)$$

$$k_d = \frac{k_{d1} + k_{d2}K_1C_M + k_{d3}K_1K_2(C_M)^2}{1 + K_1C_M + K_1K_2(C_M)^2} \quad (4)$$

Here, k_{d1}, k_{d2} and k_{d3} are the rate constants for dark ring-closure reactions for **P**, $\mathbf{P}Ca^{2+}$, and $\mathbf{P}(Ca^{2+})_2$, respectively. These equations were derived for the corresponding complexation models assuming that the concentration of uncomplexed Ca^{2+} was equal to a total $Ca(ClO_4)_2$ concentration ($[Ca^{2+}] = C_M$). This approximation is valid for a large excess of $Ca(ClO_4)_2$ over **1a** (**1b**). In our experiments, the concentrations of **1a** and **1b** were maintained at 1.5×10^{-5} mol dm^{-3}. To include the data obtained with moderate excess of $Ca(ClO_4)_2$ over **1a**, the values of C_M were corrected for the concentration of complexed Ca^{2+}, using the known K_1 value for the [**1b**·Ca^{2+}] complex. This correction is justified by the fact that only a small percentage of **1b** was converted into **P1b** upon flash photolysis with 365 nm light.

The C_M-dependent photostationary absorption spectra of **P1a** and **P1b** were analysed using the method known as principal component analysis with self-modelling[11] (PCA-SM). This analysis corroborated the supposed complexation models and provided the normalised absorption spectra of the Ca^{2+}-complexed forms of **P1a** and **P1b**.

The results of spectrokinetic studies are presented in Table 2. The formation of a weak 1 : 1 complex between **P1a** and Ca^{2+} leads to a large bathochromic effect and to a significant decrease in the rate constant for the dark ring closure of

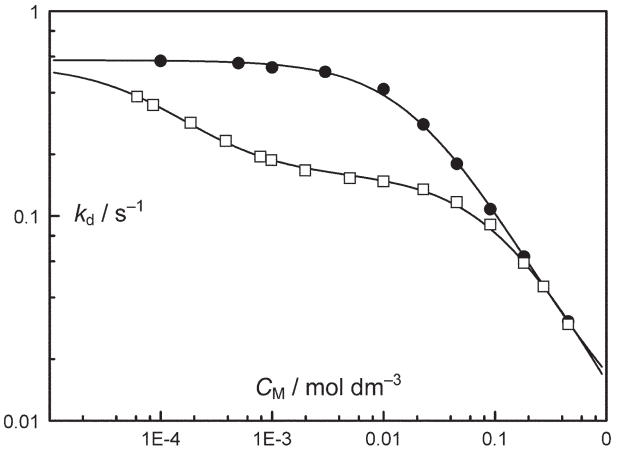

Fig. 2 Rate constant of the dark ring-closure reaction for **P1b** (squares) and **P1a** (circles) in MeCN as a function of the Ca^{2+} concentration. The solid curves are from the fits to eqn. (3) for **P1a** or to eqn. (4) for **P1b**.

P1a, indicating that the metal ion in the 1 : 1 complex [**P1a**·Ca^{2+}] is coordinated to the oxygen atom of merocyanine (Scheme 4).

In contrast, the formation of a 1 : 1 complex between **P1b** and Ca^{2+} leads to a large hypsochromic effect. For **P1b**, the decrease in the rate constant for dark ring closure upon 1 : 1 complexation is less considerable than in the case of **1a**. The 1 : 1 complex [**P1b**·Ca^{2+}] shows the spectroscopic and kinetic properties that are similar to those of the uncomplexed merocyanine form of **1c** (*i.e.* **P1c**). This indicates that the Ca^{2+} ion in this complex is coordinated to the crown ether moiety. The stability constant for the 1 : 1 complex [**P1b**·Ca^{2+}] is almost an order of magnitude lower than that for the complex [**1b**·Ca^{2+}].

In addition to the 1 : 1 complex, **P1b** is able to form a very weak 1 : 2 complex [**P1b**·$(Ca^{2+})_2$]. The 1 : 2 complex arises, most probably, due to the coordination of Ca^{2+} to merocyanine oxygen in the [**P1b**·Ca^{2+}] complex (Scheme 5).

SERS spectroscopy study of chromenes 1a,b

SERS spectra of the compounds **1a**,**b** in acetonitrile can be recorded at concentrations ranging from 5 μM to 50 mM. They are characterised by a wide set of Raman bands in the 900–1620 cm^{-1} region (Fig. 3, Table 4). The addition of $Ca(ClO_4)_2$ to a solution of **1b** induced concentration-dependent changes in the SERS spectra (Fig. 4, Table 3) corresponding to the formation of a complex between **1b** and theCa^{2+} cation.

The assignment of the SERS bands and identification of the origin of cation-induced spectral changes provided the conclusion that the SERS spectra of **1a**,**b** could be superpositions of the signals from a thermodynamically equilibrated mixture of open (coloured) and closed (colourless) forms (Scheme 3). It is known that even a very small fraction of coloured molecules

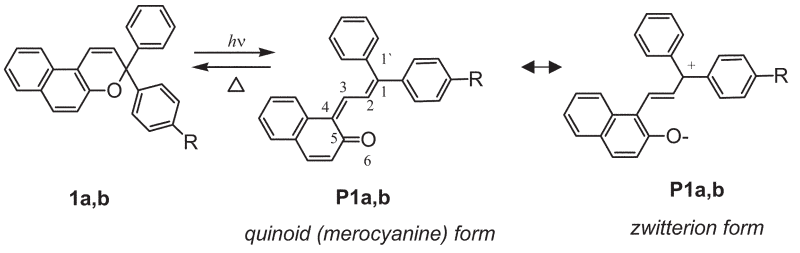

Scheme 3

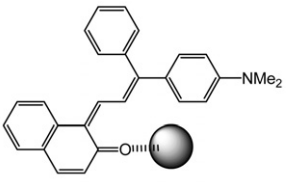

Scheme 4

can provide a dominant (or perceptible) contribution to the SERS spectrum.[12–15] This occurs due to a resonance of the excitation wavelength with the electronic transition of the molecule. Coupling of the molecular resonance with the surface plasmon resonance for the adsorbed molecules provides an additional several-fold enhancement of the Raman signal (resonance SERS effect). A trace analysis becomes possible when the resonance SERS effect is complemented with preferential adsorption of the coloured molecules on the SERS-active surface. To estimate the probable contribution of coloured species and to identify the corresponding Raman bands, the SERS spectra of free **1b** and its complex with Ca^{2+} were compared at the 457.9 and 514.5 nm excitation wavelengths (λ_{exc}). The cross sections of the vibrational modes of the **P1b**–Ca^{2+} complex should increase sharply at λ_{exc} = 457.9 nm due to the resonance with the 440 nm electronic transition (Table 2). In contrast, the SERS cross sections of **P1b** should be higher at λ_{exc} = 514.5 nm than at λ_{exc} = 457.9 457.9 nm, because of the resonance with the 543 nm absorption band (Table 2). Changes in the relative intensities of the SERS bands of coloured species have to be rather high, since the Raman cross sections at resonance excitation are known to be roughly proportional to the absorption cross section squared. In reality, none of the bands in the SERS spectra of free **1b** or its complex with Ca^{2+} were separately decreased or enhanced in the above-described manner. Instead, the intensity of the SERS spectra decreased slightly at λ_{exc} = 457.9 nm as compared with λ_{exc} = 514.5 nm (not shown). This dependence was expected for the adsorbed non-coloured species due to a decrease in the interaction between the exciting light and a surface-plasmon polariton resonance at 457.9 nm *vs.* 514.5 nm. The surface-plasmon polariton resonance is an essential factor contributing to the SERS mechanism for non-coloured species.[18] Finally, it was concluded that the open form of either free **1b** or its complex with Ca^{2+} did not contribute noticeably to the observed SERS spectra. Ethanol was used as a polar solvent facilitating the formation of the open form of merocyanine-like dyes. No changes were observed in the SERS spectrum of **1b** in ethanol as compared with that in acetonitrile (not shown), thus indicating predominance of the closed form of **1b** in both solvents. Taking into account high sensitivity of SERS spectroscopy to the merocyanine form,[14,15] the following differences between

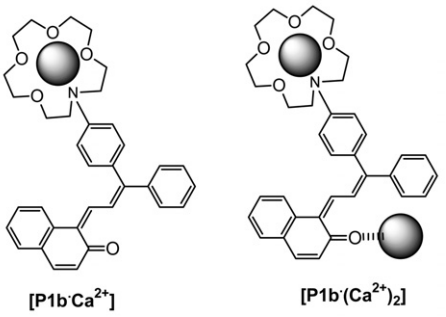

Scheme 5

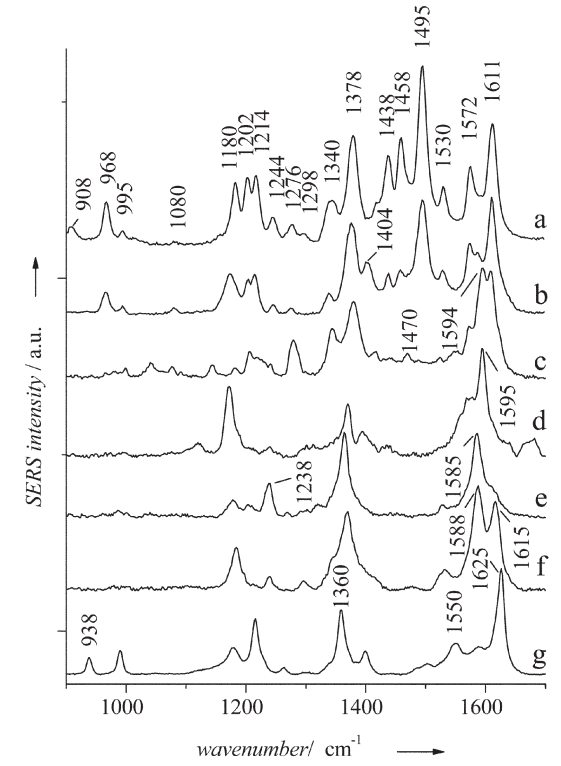

Fig. 3 SERS spectra of compounds **1b** (a), **1a** (b), **1c** (c), 4-formylphenylaza-15-crown-5 ether (d), **2b** (e), **3b** (f) and **3a** (g) in acetonitrile at λ_{exc} = 514.5 nm. The contribution of solvent bands was subtracted.

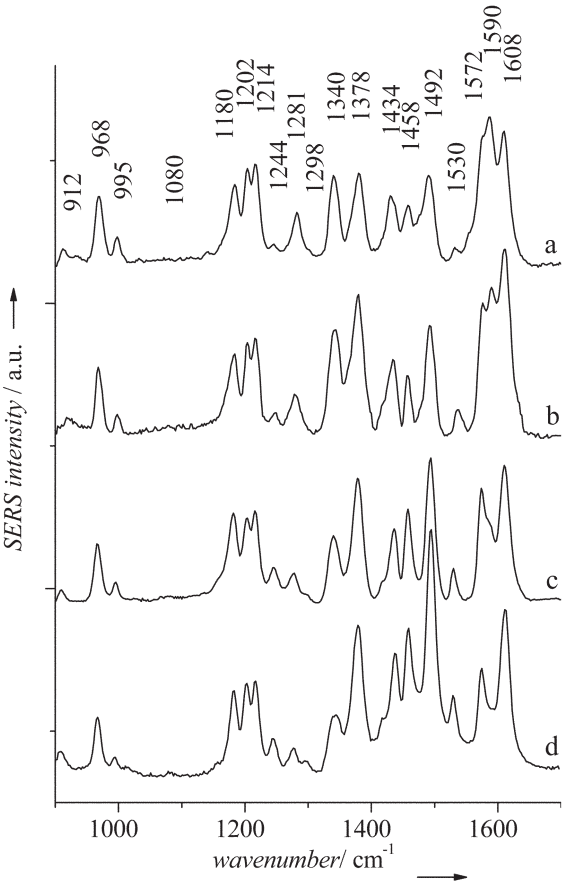

Fig. 4 SERS spectra of **1b** in acetonitrile at the different metal/ligand (M/L) molar ratios: (a) 10 : 1, (b) 3 : 1, (c) 1 : 1 and (d) free **1b**.

Table 3 Frequencies ($\Delta\nu$), relative intensities (I_{rel}) and assignments of the bands in the SERS spectra of free **1a**,**b** and the complex formed by **1b** with Ca^{2+} cations

1a		1b			
$\Delta\nu$, cm^{-1}	I_{rel}	$\Delta\nu$, cm^{-1}	I_{rel}	$I_{rel}(Ca^{2+})/I_{rel}$][b]	Assignments
908	4	*908 (+4)*[a]	8		
968	21	968	24		CH def[c] ν_{17a}[d] (pDB[e])
995	7	995	7	2.2	ring def ν_{12}(MB)
1084	5	1080	4	3.3	
1176	38	1180	37		CH def ν_{9a}(pDB)
1206	27	1202	29		DNAPH + MB
1218	34	1214	38		DNAPH + MB
1248	9	1244	15	0.5	
1276	5	*1276 (+5)*	10	1.9	DNAPH + MB
1298	4	1298	6		
1342	12	1340	19	2.4	DNAPH + MB
1378	82	1378	62		ring str & def ν_{19b}(pDB) + DNAPH + MB
1404	28				CH_3 bend + NMe_2 asym. str[17]
1440	15	*1438 (−4)*	40	0.8	
1460	15	1458	48	0.8	
1498	93	*1495 (−3)*	100	0.6	
1532	17	1530	23	0.5	ring str & def ν_{19a}(pDB)
1576	46	1572	38	1.7	ring str ν_{8b}(pDB) + DNAPH + MB
1590	27	1590	8	9.0	ring str ν_{8a}(pDB) + DNAPH + ring str ν_{8b}(MB)
1614	100	*1611 (−3)*	68		DNAPH + ring str ν_{8a}(MB)

[a] The bands that shift upon the addition of $Ca(ClO_4)_2$ are marked by italic. The value of the shift is given in parentheses. [b] Changes in the relative intensities of the bands induced by the addition of $Ca(ClO_4)_2$. Only noticeable changes are indicated. [c] Approximate description of vibration: def, deformation; str, stretch; bend, bending; asym, asymmetric. [d] Wilson notation of the vibrational modes of benzene. [e] pDB, *para*-disubstituted benzene; MB, monosubstituted benzene; DNAPH, disubstituted 3*H*-naphthopyran.

Table 4 Heat of formation ($\Delta H°_f$), dipole moment (μ) and cation affinity (CA) for free and complexed TC and TT merocyanine isomers in the gas phase and in an aqueous medium at 25 °C

		$\Delta H°_f$ (kcal mol^{-1}) μ (Debye)		CA[a] (kcal mol^{-1})
Compound		Gas	Water	
P1c				
free	TC	82.34 (2.74)	72.42 (4.38)	
	TT	84.17 (2.78)	72.23 (4.99)	
O–Mg^{2+}	TC	465.05	275.78	10.9
	TT	465.35	275.86	10.6
P1a				
free	TC	78.31 (2.01)	65.79 (3.75)	
	TT	80.11 (3.86)	65.63 (6.01)	
O–Mg^{2+}	TC	431.20	268.81	14.24
	TT	431.17	272.90	6.99
N–Mg^{2+}	TC	466.02	286.19	6.14
	TT	472.07	286.51	6.62
P1b				
free	TC	−71.25 (1.94)	−92.37 (3.64)	
	TT	−69.44 (3.72)	−92.57 (6.24)	
O–Mg^{2+}	TC	278.07	111.47	12.60
	TT	277.96	111.75	13.04
Crown-ether-Mg^{2+}	TC	254.02	107.48	16.59
	TT	263.49	107.16	17.63
O–Mg^{2+}, Crown-ether-Mg^{2+}	TC	790.75	311.50	26.83
	TT	788.95	312.35	26.7

[a] calculated in an aqueous medium.

compound **1b** and the previously studied azacrown-containing spironaphthoxazine[14,15] should be mentioned: the equilibrium between the open and closed forms of **1b** is totally shifted to the closed formin acetonitrile, while a polar solvent (ethanol) environment or complex formation with the Ca^{2+} cation does not shift the equilibrium toward the open form.

The SERS spectra of **1a**,**b** are rather similar in appearance but distinguished in details (Fig. 3). Besides, they differ considerably from the spectrum of the parent compound **1c** (Fig. 3). The differences between the SERS spectra of **1a** and **1b** include small shifts (2–4 cm^{-1}) of several bands and noticeable changes in the relative intensities of bands in the 1230–1620 cm^{-1} region (Table 3). Moreover, the 1404 cm^{-1} band of **1a** is not observed in the spectrum of **1b**. One would expect that the changes in the 1230–1500 cm^{-1} region are directly related to the vibrations of the azacrown ether moiety. In particular, CH_2 twisting, wagging and scissoring modes are known to contribute to the 1230–1300 cm^{-1}, 1340–1440 cm^{-1} and 1445–1500 cm^{-1} regions, respectively, in the normal Raman spectrum of a crown ether.[16] Nevertheless, it was not the case for the SERS spectrum of **1b**. While analysing the SERS spectra of azacrown-containing compounds **3b**, 4-formylphenylaza-15-crown-5 ether, **2b** (Fig. 3) and compound **3a**, it was concluded that no specific bands related to the crown-ether vibrations were enhanced. Instead, definite sets of bands of substituted benzene were mainly observed. Appearance of the band at *ca.* 1404 cm^{-1} in the spectra of **1a** and **3a** as compared with the spectra of **1b** and **3b**, respectively, allowed us to assign this band to vibrations of the dimethylamino group of **1a** and **3a**. Supporting this conclusion, the band at *ca.* 1404 cm^{-1} was reasonably absent from the SERS spectra of **1c**, **2b** or 4-formylphenylaza-15-crown-5 ether (Fig. 3). This may be the NMe_2 asymmetric stretching mode as follows from calculations of the vibration wavenumbers and SERS spectrum analysis of coumarin 152.[17]

It was concluded that the origin of the vibrational modes contributing to the spectra of both **1a** and **1b** was the same, except for the 1404 cm^{-1} band, and the relative intensities changed due to some alteration in the adsorption geometry of the molecule induced by the bulky azacrown substituent. It is well known that the vibration mode activities and intensities in SERS spectra might depend considerably on the molecular orientation on the metal surface.[19]

Accordingly, the SERS spectra of **1a** and **1b** seem to be superpositions of the bands of the disubstituted 3*H*-naphthopyran (DNAPH), *para*-disubstituted benzene (pDB) and monosubstituted benzene (MB) chromophores. Exact assignment of these bands is complicated at present, but their qualitative classification can be done due to a comparative analysis of the spectra of **1c, 3a,b, 2b** and 4-formylphenylaza-15-crown-5 ether (Fig. 3). The band at *ca.* 1180 cm^{-1} was observed in the spectra of **1a**, **1b**, **3a**,**b** and 4-formylphenylaza-15-crown-5 ether, but not in the spectra of **1c** or **2b**; this allowed assigning this band to the ν_{9a} CH deformation mode of pDB. The ν_{19b}, ν_{8b} and ν_{8a} ring stretching modes of pDB contributed, at least partially, to the 1378, 1576 (1572) and 1590 cm^{-1} bands of the **1a**,**b**, respectively. The 1206 (1202), 1218 (1214), 1276, 1342 (1340) and 1614 (1611) cm^{-1} bands seemed to originate from the vibrational modes of the DNAPH and/or MB chromophores. Besides, DNAPH and/or MB chromophores contributed to the 1378, 1576 (1572) and 1590 cm^{-1} bands of **1a**,**b**.

Sers titration of 1b with $Ca(ClO_4)_2$

The intensity ratio R of the 1590 and 1572 cm^{-1} bands was found to be well suited for monitoring the complexation between **1b** and Ca^{2+}. This ratio was equal to $R_f = 0.2$ for free **1b**, increased during titration of the ligand with $Ca(ClO_4)_2$ up to $R_c = 1.35$ and no longer changed on further increase in the Ca^{2+}/**1b** ratio. Thereby the R value was measured to estimate the relative amount of complexes (α) in the course of the SERS titration procedure.

As discussed above, the nitrogen atom of the azacrown ether fragment produces the electron-donating effect to the conjugated benzene ring, whereas the coordination of Ca^{2+} to the crown ether ring diminishes it. This can induce noticeable changes in the pattern of relative intensities of the Raman-active vibrations of pDB. Alternatively, orientation of the complex [**1b**·Ca^{2+}] on the silver surface can be different in part from that of free **1b** and result in the observed spectral features.

In strict accordance with the SERS titration procedure developed earlier,[20] the relative amount of complexes (α) in the solution was defined at the given Ca^{2+}/**1b** molar ratio as

$$\alpha = (1 + \theta F(R_c - R)/(R - R_f))^{-1}, \quad (5)$$

where F is the ratio of the intensity of the 1572 cm^{-1} band at complete **1b** complexation to the intensity of the 1572 cm^{-1} band of the free ligand; θ is the ratio of the adsorption coefficient of the complex to that of free **1b**. The F ratio was equal to 0.61 ± 0.07. This value was determined from the SERS spectra of free **1b** and its complex with Ca^{2+} recorded under fixed experimental conditions with a constant concentration of the ligand as the average of three independent pairs of measurements.

The factor θ provided a correction for the different adsorption efficiency of free **1b** and its complex with Ca^{2+} at the SERS-active surface. The θ value was estimated following the formalism of the Langmuir adsorption theory as described elsewhere:[21]

$$\theta = F_{lin}/F_{sat}, \quad (6)$$

where $F_{lin}$and $F_{sat}$are the F values measured at **1b** concentrations corresponding to the linear (5–100 μM) and saturation (1–50 mM) regions of the Langmuir adsorption isotherm (not shown), respectively. The θ value of 0.21 ± 0.06 indicates a preferential adsorption of free **1b** as compared to its complex with Ca^{2+} cations.

The isotherm of Ca^{2+} binding to **1b** derived from the SERS titration experiments was analysed by the Scatchard model.[21] The linear form of the Scatchard graph and its slope (not shown) corresponded to the 1 : 1 complex [**1b**·Ca^{2+}]. The association constant determined from the SERS titration data (log $K_1 = 4.6 \pm 0.3$) was found to be rather similar to that estimated from spectrophotometric data (Table 2), providing an independent validation for the proposed complexation scheme.

Molecular orbital calculations

The photomerocyanines can ultimately adopt either *trans-cis* (TC) or *trans-trans* (TT) molecular conformation (Fig. 5). To reveal the preferential conformation, the stabilities of these isomers were estimated using the PM3[22] method of molecular geometry optimisation. In the gas phase, the TC isomers of photomerocyanines **P1a**, **P1b** and **P1c** were found to be 1.8 kcal mol^{-1} more stable than the TT isomers (Table 4).

The allowance for solvent effect[23] decreased the heat of formation of both isomers (Table 4). This decrease was observed for all the molecules, but most remarkably, for **P1b**. The solvent effect was even greater for the TT isomer and, surprisingly, both isomers had approximately the same stability in an aqueous medium (Table 4). However, the TT isomers were found to deviate strongly from a planar structure due to steric repulsion between the naphthalene moiety and the H(3) hydrogen of the conjugated chain (Fig. 5). As a consequence, the TT isomer was less conjugated and, therefore, a less probable candidate for being responsible for the strong merocyanine absorption in the visible region than the TC isomer. Accordingly, excited states were calculated only for the TC merocyanine conformers (Table 6).

Two sites in **P1a**, the amino-group nitrogen atom and merocyanine oxygen, are suitable for complexation with a metal cation. In the case of **P1b**, these sites are the azacrown-ether moiety and merocyanine oxygen.To determine the thermodynamically preferential site of complexation, the cation affinity (CA) was calculated for each site at 298 K as a value opposite in sign to the enthalpy change ΔH°_f(rxn) in the reaction:

$$\mathbf{P} + Mg^{2+} \rightarrow \mathbf{P}Mg^{2+} \quad (7)$$

$$CA(\mathbf{P}) = -\Delta H^\circ_f(rxn) = \Delta H^\circ_f(Mg^{2+}) + \Delta H^\circ_f(\mathbf{P}) - \Delta H^\circ_f(\mathbf{P}Mg^{2+}), \quad (8)$$

where $\Delta H^\circ_f(Mg^{2+})$, $\Delta H^\circ_f(\mathbf{P})$ and $\Delta H^\circ_f(\mathbf{P}Mg^{2+})$ are the heats of formation of the Mg^{2+} cation, free P, and its complex with Mg^{2+}, respectively. $\Delta H^\circ_f(Mg^{2+})$ was calculated to be 214.26 kcal mol^{-1} in an aqueous medium. The Mg^{2+} cation was considered, instead of the Ca^{2+} cation, because its PM3 Hamiltonian was known both in the gas phase and in an aqueous medium. For comparison of the calculation results with the obtained experimental data, one may assume that the electronic effects of both cations are roughly similar.

In the case of **P1a**, the highest CA value was obtained for merocyanine oxygen of the TC isomer (Table 4). The interaction of Mg^{2+} with oxygen in TC isomer produced a complex that was considerably (by 18 kcal mol^{-1}) more stable than the TT complexes and 4 kcal mol^{-1} more stable than the TC complex formed by Mg^{2+} with the amino group. This finding is consistent with the previous studies reported on merocyanines.[23] The involvement of the solvent effect was important to reveal the most stable conformation, because the merocyanine oxygen complexes of both isomers in the gas were equally stable (Table 4).

In the case of **P1b**, the most favourable site for complexation with Mg^{2+} was the crown-ether moiety (Table 4). The CA value for this site was 4 kcal mol^{-1} higher than that for merocyanine oxygen. At the same time, it was difficult to indicate the preferential conformation of the complex, since the stabilities of the TC and TT complexes were approximately equal (Table 4). Similarly, when the formation of the 1 : 2 complex [**P1b**·$(Mg^{2+})_2$] was considered, the CA values and the complex stabilities were calculated to be equal for the TT and TC conformers (Table 4).

Optimized geometries. It is generally accepted that the merocyanine π-electronic structure can exist as either a neutral non-polar quinoid form or a charge-separated (zwitterionic) form (Scheme 3), but, definitely, some intermediate states are also possible. Due to changes in the equilibrium between these two forms, the merocyanines possess peculiar structural and optical properties. As a first approximation, the change in the molecular geometry on passing between the quinoid and zwitterionic forms could be indexed by bond length alternation (BLA).[24] For the compounds under study, the BLA index was calculated as the difference between the length of the C2–C3 bond and the average length of the C1–C2 and C3–C4 bonds. A positive BLA value indicates that the C2–C3 bond length is longer than the average length of the C1–C2 and C3–C4 bonds and corresponds to the quinoid-like form. A negative BLA value corresponds to the zwiterionic structure. The main molecular geometry parameters calculated at the semi-empirical level are presented in Table 5.

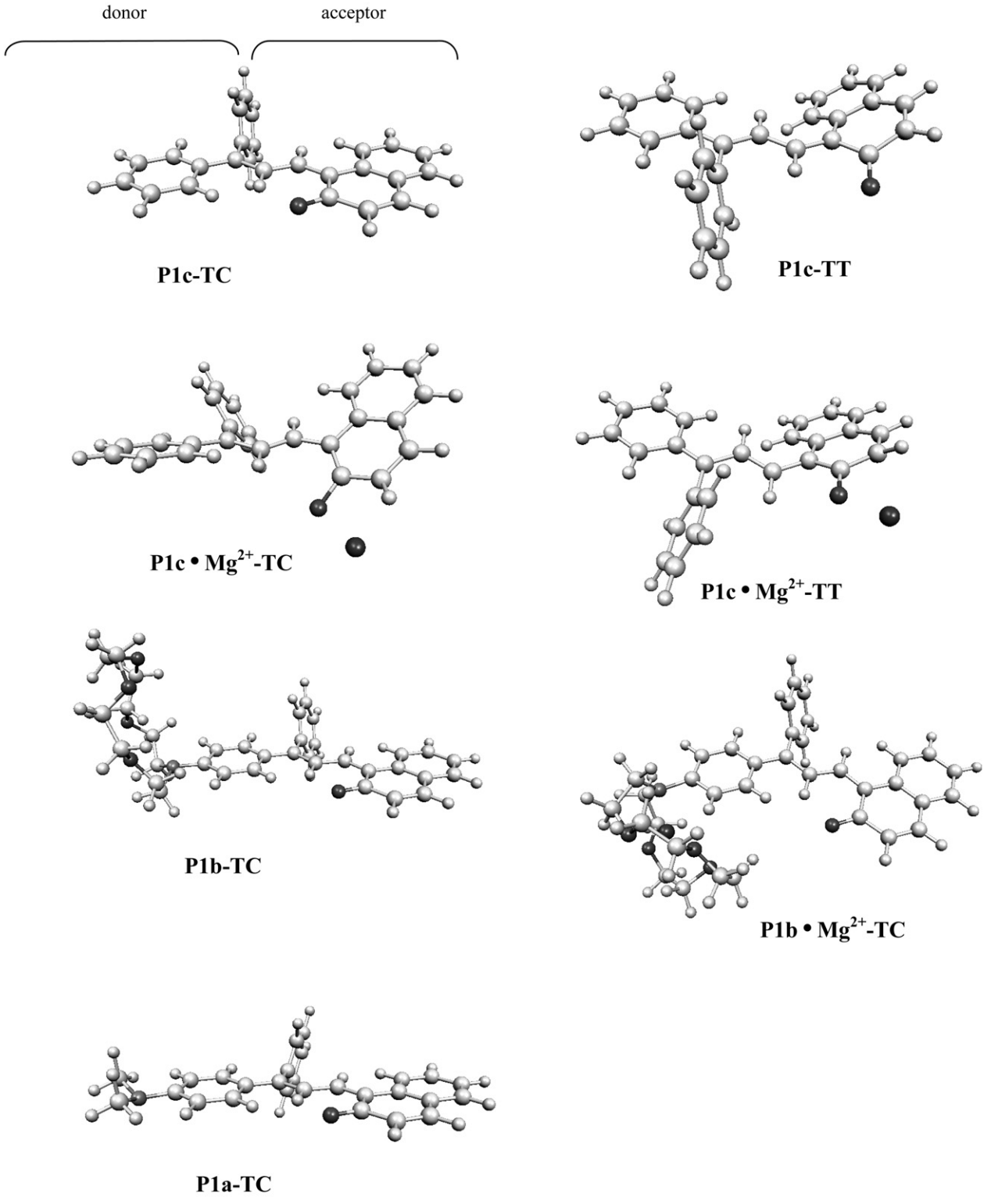

Fig. 5 Selected optimised structures for free, O-complexed and crown-ether complexed TC and TT isomers of **P1a**, **P1b** and **P1c**.

According to these calculations, the TC isomers of merocyanines in the gas phase were found to be planar (C_s point group of symmetry) and to adopt the quinoid rather than zwitterionic form. The BLA index changed only slightly when the solvent effect was taken into account, indicating that the solvent reaction field was not strong enough to induce the appreciable geometric distortion in the conjugated system of the merocyanine. In contrast, the charge distribution was highly affected by the solvent effect as followed from the considerable increase in the dipole moment values as compared with the gas phase data (Table 4).

The NMe_2 or crown-ether substituents had a very weak influence on the lengths of the conjugated bridge bonds (Table 5). However, as anticipated, the effect of substituents on the electron density was pronounced and depended on the extent of conjugation between the lone pair of electrons of the nitrogen atom and the π-electronic system of the benzene ring. Indeed, orientation of the substituent group with respect to the benzene ring, *i.e.* planar or twisted, results from a delicate balance between involvement of the *N*-phenyl group in conjugation and steric repulsion. The conjugation of the *N*-phenyl group favoured a planar conformation, whereas steric

Table 5 Lengths of the conjugated chain bonds (Å) and the bond length alternation (BLA) parameter for the TC isomers of **P1a**, **P1b** and **P1c** and their complexes with mg^{2+} cation

	C1′–C1	C1–C2	C2–C3	C3–C4	C4–C5	C5–O6	BLA
P1c							
Free	1.449	1.388	1.412	1.395	1.485	1.230	0.0205
[**P1c**·Mg^{2+}]	1.424	1.434	1.365	1.444	1.414	1.354	−0.074
P1a							
Free	1.446	1.389	1.411	1.395	1.485	1.230	0.019
[**P1a**·Mg^{2+}]	1.438	1.401	1.412	1.397	1.470	1.279	0.013
P1b							
Free	1.446	1.389	1.411	1.395	1.485	1.230	0.019
[**P1b**·Mg^{2+}]	1.444	1.391	1.408	1.400	1.490	1.234	0.0125
[**P1b** ·Mg^{2+}]$_2$	1.460	1.389	1.419	1.392	1.449	1.322	0.0285

repulsion between the methyl groups of the NMe_2 substituent and phenyl hydrogen atoms promoted a twisted geometry. The conjugation effect was strong enough to provide the planar conformation for free **P1b** and even for free **P1a** in the gas phase as well as in aqueous media (Fig. 5). In order to estimate the electron-donating effect of nitrogen, the merocyanine molecule was formally sub-divided into two moieties: the donor and acceptor ones (Fig. 5). The charge distribution between the donor and acceptor moieties of **P1c** was +0.07 e and −0.07 e, respectively. The nitrogen atom induced a small charge displacement toward the acceptor moiety, thus providing +0.085 e and −0.085 e for the donor and acceptor moieties, respectively.

Complexation of Mg^{2+} with merocyanine oxygen of **P1c** affected significantly the molecular geometry, as follows from the decrease in the BLA index (Table 5). The BLA index for the complex [**P1c**·Mg^{2+}] was negative, pointing to the zwitterionic form of the molecule (Table 5). The calculated C5–O6 bond length (1.354 Å) was slightly shorter than the C–O bond length in phenol (1.364 Å), while the C2–C3 bond length (1.365 Å), was comparable to the double bond length in ethylene (1.34 Å). Complexation of Mg^{2+} with merocyanine oxygen of **P1a** induced less pronounced changes in the bond lengths, and the [**P1a**·Mg^{2+}] complex retained the quinoid form. Complexation of Mg^{2+} with the crown ether moiety of **P1b** eliminated conjugation of the *N*-phenyl group, and, as a result, the crown ether substituent turned by 90° relative to the benzene ring plane (Fig. 5). The [**P1a**·Mg^{2+}] complex exists in the quinoid form (Table 5).

Excited states calculations. Table 6 lists the calculated maxima of the long-wavelength electronic transition of merocyanines **P1a**, **P1b** and **P1c**, which deviate from the experimental values by less than 10% in the case of the aqueous medium approximation. It is seen that all merocyanines exhibit a slight positive solvatochromism.[25] This behaviour can be rationalised qualitatively by the fact that the ground state dipole moment regularly increases upon excitation (Table 6).

Table 6 Calculated electronic transition maxima (λ_{max}, nm), oscillator strengths (OS) and dipole moments of the ground (μ_{S0}, in Debye) and first excited singlet (μ_{S1}, in Debye) states for the TC isomers of **P1a**, **P1b** and **P1c** as well as for their complexes with Mg^{2+} cations

	Gas phase				Aqueous medium	
	λ_{max}	OS	μ_{S0},	μ_{S1}	λ_{max}	OS
P1a	467.4	0.91	1.80	6.84	496.5	0.94
[**P1a**·Mg^{2+}]	580.5	0.98			620.2	1.07
P1b	469.6	0.92	1.45	6.49	507.9	0.92
[**P1b**·Mg^{2+}]	450.0	0.69			452.7	0.78
[**P1b**·(Mg^{2+})$_2$]	563.9	0.47			496.6	0.79
P1c	427.3	0.76	2.17	3.26	446.5	0.68
[**P1c**·Mg^{2+}]	491.8	0.51			619.2	0.65

The calculations of configurational interaction (CI) revealed that in all cases studied, the major (90–95%) contribution to the $S_0 \rightarrow S_1$ transition is made by the configuration arising from single-electron transfer from the highest occupied molecular orbital (HOMO) to the lowest unoccupied molecular orbital (LUMO). Therefore, it was reasonable to analyse the long-wavelength electronic transitions of the merocyanines in terms of their HOMO and LUMO. The HOMO and LUMO of the molecules **P1a** and **P1c** are depicted in Fig. 6.

Analysis of HOMO and LUMO charge densities revealed a substantial difference between free and complexed merocyanines **P1a** and **P1b**. The degree of charge transfer upon HOMO-LUMO excitation can be estimated by calculating the total charge gained (lost) by the acceptor (donor) moiety of the molecule. Fig. 6 illustrates how the total π-electron density is distributed between the donor and acceptor fragments of each molecule in the HOMO and LUMO. Thus, in the case of HOMO state of free **P1c**, 46% of the charge belongs to the donor, leaving 54% for the acceptor moiety. The situation is enhanced in the LUMO state, where the charge is distributed as 33% and 67% between the donor and acceptor fragments. The charge transfer for the long-wavelength transition is 13% (46% minus 33% or 67% minus 54%) of the charge available in the molecular orbital. The same estimation for **P1a** revealed that 33% of the available charge was transferred from the donor to the acceptor moiety. Complexation of Mg^{2+} with merocyanine oxygen increased the charge transfer to 66% and to 70% for **P1c** and **P1a**, respectively. Therefore, the [**P1a**·Mg^{2+}] and [**P1c**·Mg^{2+}] complexes can be considered as intramolecular charge transfer complexes.

The NMe_2 group or the crown ether moiety act as donor substituents and induce a bathochromic shift of the long-wavelength absorption maximum as compared with the **P1c** absorption maximum (Tables 2, 6). This shift originates mainly from the increase in the energy of HOMO (−7.86 eV for **P1a** *vs.* −8.18 eV for **P1c**), while the LUMO energy remains almost unchanged (−1.49 eV for **P1a** *vs.* −1.39 eV for **P1c**, Fig. 6). According to both calculated and experimental data (Tables 2, 6), complexation of metal cation with the crown-ether site of **P1b** gives a strong hypsochromic shift of the absorption maximum, which approaches the maximum for the unsubstituted merocyanine **P1c**. This result is consistent with the above-described loss of conjugation of the *N*-phenyl ring upon complex formation. Complexation of the second metal cation with the merocyanine oxygen polarises the molecule as a whole and induces a bathochromic shift of the absorption maximum in a similar way as is done by substituents in **P1b** and **P1a** as compared with **P1c**.

In conclusion, the complex formation and the photochromic behaviour of the novel azacrown-containing chromene and its crown-free analogue were studied in detail. According to the experimental data and the results of molecular orbital calculations, the crown ether moiety is a preferable site of binding to metal cations for both the closed and open forms of chromene **1b**. The spectroscopic behaviour of chromenes **1a**,**b** is strongly affected by the complexation with Ca^{2+}. Metal cation binding to the crown ether moiety of **P1b** or to merocyanine oxygen of **P1a** preserves the quinoid merocyanine form, whereas its binding to merocyanine oxygen of **P1c** changes the molecular structure towards the zwitterionic form. The photocontrolled formation of merocyanine leads to a noticeable decrease in the ability of **1b** to bind Ca^{2+}. In contrast, the dimethylamino-substituted chromene **1a**, which is unable to bind Ca^{2+} in the dark, possesses a low Ca^{2+}-binding ability upon UV irradiation.

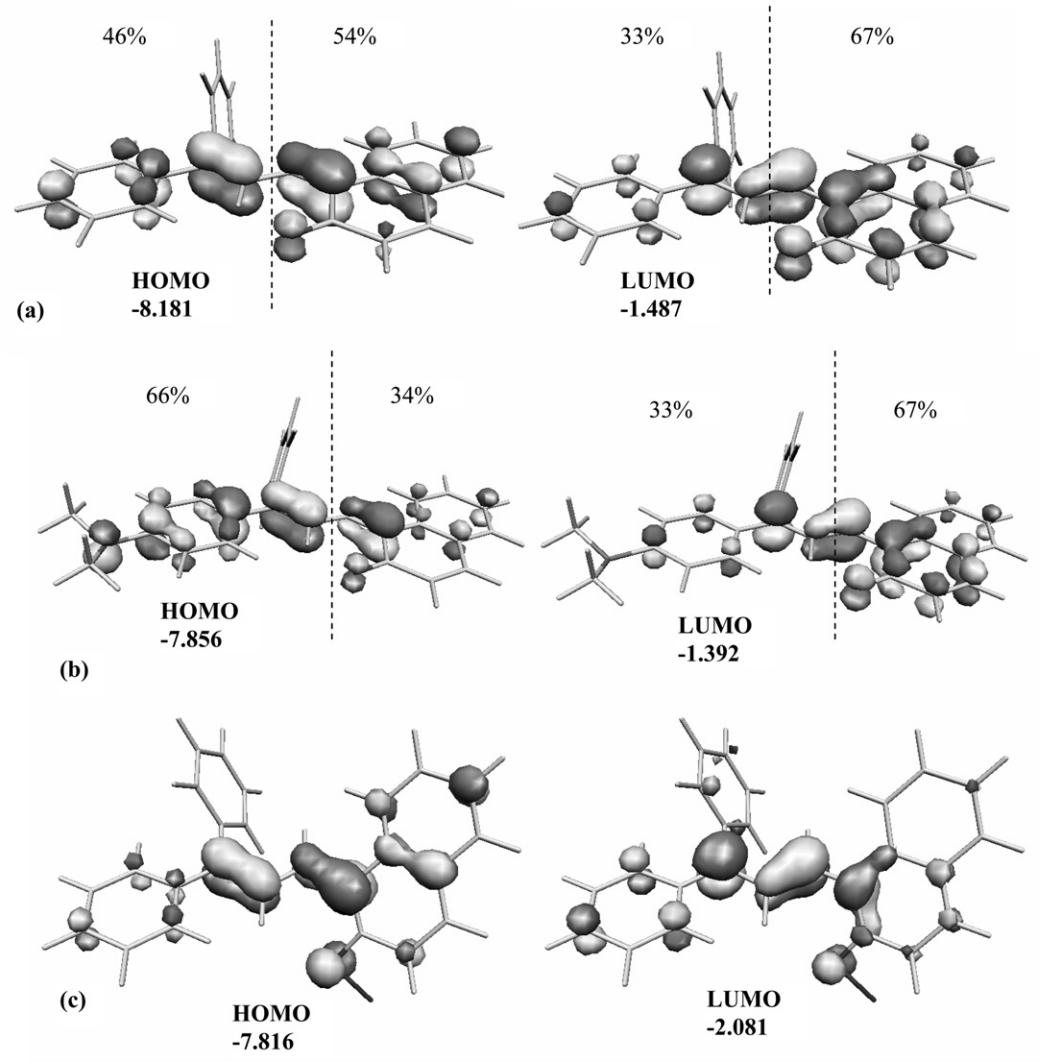

Fig. 6 Three dimensional representation and energies (in eV) of the HOMO and LUMO for **P1b** (a), **P1a** (b) and O-complexed **P1c** (c). The percentages of charge distributions between the donor and acceptor moieties are also indicated for **P1b** and **P1a**.

Experimental section

Methods and materials

^{1}H NMR spectra were recorded on Bruker DRX-500 spectrometers using TMS as an internal standard and MeCN-d_3 as a solvent. The chemical shifts and the spin–spin coupling constants were determined with an accuracy of 0.01 ppm and 0.1 Hz, respectively. To prove the structure of complexes the COSY and NOESY 2D spectra were recorded using the standard Bruker pulse sequences (cosy45, cosygs, noesytp, roesyprtp) and processed using the *XWINNMR* program. The mixing time for the NOESY spectra was 700 ms, the delay between the experiments was 2 s, and the number of scans per experiment was 32. A total of 512 f1 points and 2048 f2 points were accumulated. Mass spectra were obtained using a Varian MAT 311A instrument with an ionisation energy of 70 eV. TLC analysis was carried out using DC-Alufolien Kieselgel 60 F_{254} (Merck) and DC-Alufolien Aluminiumoxid 60 F_{254} neutral (Typ E) plates. For column chromatography, silica gel 60 with a particle size of 0.063–0.200 mm and Aluminiumoxid 150 basisch (Typ T) were used.

Benzanilide, *N*,*N*-dimethylaniline (**2a**), *N*-phenylaza-15-crown-5 ether (**2b**), complex LiC≡CH·$NH_2CH_2CH_2NH_2$, 2-naphthol and *p*-toluenesulfonic acid (all from Aldrich) were used as received. Chromene **1c** was prepared according to the known procedure.[7]

Synthesis

Synthesis of the ketones 3a,b. 2 mmol of $POCl_3$ was added dropwise with stirring to a mixture of 1 mmol of benzanilide and 2 mmol of *N*,*N*-dimethylaniline **2a** or *N*-phenylaza-15-crown-5 ether **2b**. The reaction mixture was kept for 4 h at 100 °C and dissolved in hot 17–18% HCl. The solution was filtered to remove the orange precipitate, treated with 10% NaOH, and extracted with benzene. Evaporation of organic solvent and column chromatography (silica gel, eluent heptene : ethylacetate, 2 : 1 to 1 : 3) afforded **3a**,**b**.

(4-Dimethylaminophenyl)phenylmethanone (3a). Yield 23% (recrystallised from heptane), m.p. 86–88 °C.[26]

Phenyl-[4(1,4,7,10-tetraoxa-13-aza-cyclopentadec-13-yl)-phenyl]-methanone (3b). Yield 28% (recrystallized from heptane), m.p. 90–92 °C; ^{1}H NMR (ppm, *J* Hz, $CDCl_3$, 25 °C): δ = 3.64 (s, 8 H, $4CH_2O$), 3.68 (m, 8 H, $4CH_2O$), 3.80 (m, 4 H, $2CH_2O$), 6.68 (d, 2 H, H-2′, *J* = 9.1), 7.46 (t, 2 H, H-2, *J* = 7.4), 7.53 (t, 1 H, H-3, *J* = 7.3), 7.73 (d, 2 H, H-1, *J* = 8.4), 7.78 (d, 2 H, H-1′, *J* = 9.00). MS (70 eV, EI): *m*/*z* (%): 399 (87) $[M]^+$, 266 (48), 254 (54), 224 (55), 223 (49), 210 (83), 132 (68), 105 (100), 77 (74), 58 (35); elemental analysis calcd (%) for $C_{23}H_{29}NO_5$ (399.5): C 69.15, H 7.30, N 3.54; found C 69.21, H 7.44, N 3.55.

Synthesis of the propyn-1-ols 4a,b. A solution of 1 mmol of ketone **3a** or **3b** in anhydrous tetrahydrofuran was added over a period of 1 h with stirring at 60 °C to 5 mmol of the complex

LiC≡CH·$NH_2CH_2CH_2NH_2$ in anhydrous tetrahydrofuran. The reaction mixture was kept at the same temperature for 2 h, cooled to room temperature and extracted with benzene. The residue was washed with water and extracted with ethyl acetate. Evaporation of ethyl acetate and purification of the product by extraction with hexane afforded **4a**,**b**.

1-(4-Dimethylaminophenyl)-1-phenyl-2-propyn-1-ol (4a). Yield 53% m.p. 150–152 °C; ^{1}H NMR (ppm, *J* Hz, $CDCl_3$, 25 °C): δ = 2.73 (s, 1 H, OH), 2.86 (s, 1 H, CH), 2.95 (s, 6 H, 2Me), 6.68 (d, 2 H, H-5, *J* = 8.9), 7.28 (t, 1 H, H-3), 7.34 (t, 2 H, H-2, *J* = 7.8), 7.45 (d, 2 H, H-4, *J* = 8.9), 7.62 (d, 2 H, H-1, *J* = 7.2); MS (70 eV, EI): *m*/*z* (%): 251 (26) $[M]^+$, 250 (35), 234 (23), 226 (37), 225 (47), 174 (26), 148 (100), 134 (24), 105 (79), 77 (91); elemental analysis calcd (%) for $C_{16}H_{17}NO$ (239.3): C 80.30, H 7.16, N 5.85; found C 80.54, H 6.88, N 5.84.

1-Phenyl-1-[4-(1,4,7,10-tetraoxa-13-aza-cyclopentadec-13-yl)-phenyl]-prop-2-yn-1-ol (4b). Yield 75%, m.p. 150–152 °C; ^{1}H NMR (ppm, *J* Hz, $CDCl_3$, 25 °C): δ = 2.67 (s, 1 H, OH), 2.84 (s, 1 H, CH), 3.58 (t, 4 H, $2CH_2O$), 3.63 (s, 8 H, $4CH_2O$), 3.67 (m, 4H, $2CH_2O$), 3.74 (m, 4 H, $2CH_2O$), 6.61 (d, 2 H, H-5, *J* = 8.9), 7.28 (t, 1 H, H-3), 7.34 (t, 2 H, H-2, *J* = 7.5), 7.39 (d, 2 H, H-4, *J* = 8.9), 7.63 (d, 2 H, H-1, *J* = 7.2); MS (70 eV, EI): *m*/*z* (%): 425 (15) $[M]^+$, 399 (96), 266 (59), 236 (55), 224 (63), 223 (58), 210 (82), 132 (74), 105 (100), 77 (83), 58 (35); elemental analysis calcd (%) for $C_{25}H_{31}NO_5$ (425.5): C 70.57, H 7.34, N 3.29; found C 70.65, H 7.71, N 3.21.

Synthesis of the chromenes 1a,b. A mixture of 1 mmol of **4a** or **4b**, 1 mmol of 2-naphthol and 0.1 mmol of *p*-toluenesulfonic acid in dry toluene was stirred for 3 h at 60 °C. Then the reaction mixture was washed with water and the organic phase was separated. After evaporation of toluene, the products **1a**,**b** were isolated by column chromatography (aluminiumoxid basisch, eluent benzene : ethylacetate 3 : 1).

3-(4-Dimethylaminophenyl)-3-phenyl-3H-naphtho[2,1-b]pyran (1a). Yield 17%, m.p. 174–176 °C; ^{1}H NMR (ppm, *J* Hz, $CDCl_3$, 25 °C): δ = 2.92 (s, 6 H, NMe_2), 6.25 (d, 1 H, H-2, *J* = 9.95), 6.66 (d, 2 H, 2H-3″, *J* = 8.9), 7.19 (d, 1 H, H-5, *J* = 8.8), 7.24 (t, 1 H, H-4′), 7.27 (d, 2 H, 2H-2″), 7.32 (m, 4 H, 2H-3′, H-1, H-8), 7.45 (t, 1 H, H-9), 7.51 (d, 2 H, 2H-2′, *J* = 8.0), 7.64 (d, 1 H, H-6, *J* = 8.6), 7.71 (d, 1 H, H-7, *J* = 8.1), 7.96 (d, 1 H, H-10, *J* = 8.5); MS (70 eV, EI): *m*/*z* (%): 377 (100) $[M]^+$, 376 (29), 301 (16), 300 (89), 257 (34), 234 (18), 209 (12), 165 (16), 150 (17), 77 (12); elemental analysis calcd (%) for $C_{27}H_{23}NO$ (377.5): C 85.91, H 6.14, N 3.71; found C 85.84, H 6.18, N 3.84.

13-[4-(3-Phenyl-3H-benzo[f]chromen-3-yl)-phenyl]-1,4,7,10-tetraoxa-13-aza-cyclopentadecane (1b). Yield 19%, m.p. 90–94 °C; ^{1}H NMR (ppm, *J* Hz, MeCN-d_3, 25 °C): δ = 3.49 (m, 4 H, $2CH_2O$), 3.53 (m, 4 H, $2CH_2O$), 3.56 (m, 8 H, $4CH_2O$), 3.64 (m, 4 H, $2CH_2O$), 6.42 (d, 1 H, H-2, *J* = 9.9), 6.63 (d, 2 H, 2H-3″, *J* = 6.96), 7.22 (d, 1 H, H-5, *J* = 8.88), 7.26 (d, 2 H, H-2″, *J* = 6.94), 7.27 (m, 1 H, H-4′), 7.36 (m, 3 H, H-8, 2H-3′), 7.38 (d, 1 H, H-1, *J* = 9.67), 7.52 (m, 1 H, H-9), 7.53 (d, 2 H, 2H-2′, *J* = 8.07), 7.74 (d, 1 H, H-6, *J* = 8.82), 7.79 (d, 1 H, H-7, *J* = 8.26), 8.03 (d, 1 H, H-10, *J* = 8.46); MS (70 eV, EI): *m*/*z* (%): 551 (100) $[M]^+$, 550 (7), 474 (26), 376 (11), 362 (14), 356 (8), 257 (34), 255 (7), 120 (9), 58 (18); elemental analysis calcd (%) for $C_{35}H_{37}NO_5$ (551.7): C 76.20, H 6.76, N 2.54; found C 76.31, H 6.67, N 2.58.

NMR spectrum of the complex of 1b with $Ca(ClO_4)_2$

A solution of **1b** (0.1 mmol) and $Ca(ClO_4)_2$ (0.1 mmol) in 0.5 mL of MeCN-d_3 was analysed by NMR spectroscopy: ^{1}H NMR (ppm, *J* Hz, 25 °C): δ = 3.33 (m, 4 H, $2CH_2O$), 3.82 (m, 8 H, $4CH_2O$), 3.87 (m, 4 H, $2CH_2O$), 3.91 (m, 4 H, $2CH_2O$), 6.55 (d, 1 H, H-2, *J* = 9.88), 7.22 (d, 2 H, H-5), 7.30 (m, 1 H, H-4′), 7.31 (d, 2 H, H-3″, *J* = 8.81), 7.38 (d, 2 H, H-3′, *J* = 7.49), 7.39 (m, 3 H, H-8, 2H-3′), 7.45 (d, 1 H, H-1, *J* = 9.92), 7.53 (t, 1 H, H-9, *J* = 8.32, *J* = 8.38), 7.57 (d, 2 H, 2H-2′, *J* = 7.62), 7.59 (d, 2 H, 2H-2″ *J* = 9.0), 7.79 (d, 1 H, H-6, *J* = 8.7), 7.81 (d, 1 H, H-7, *J* = 7.81), 8.04 (d, 1 H, H-10, *J* = 8.55).

UV/Vis spectroscopy and kinetic measurements

UV/Vis absorption spectra were recorded with a Specord M40 spectrophotometer.

The dark lifetimes of photomerocyanines **P1a**,**b** were measured using an experimental setup with a xenon flash lamp. The probing light from a KGM-100 tungsten filament lamp passed through the sample in a 1 cm quartz cell and an MDR-3-type monochromator, and struck a FEU-79 photomultiplier. After an U7-1 amplifier and an analog-digital converter, the signal entered a PC. The decay kinetics was monitored at the absorption maximum of photomerocyanine or its Ca^{2+}-complexed form. The time resolution was less than 1 ms.

The photostationary absorption spectra of merocyanine isomers were measured with the same setup upon steady-state irradiation of solutions with glass-filtered 365 nm light of a DRSh-1000 high-pressure mercury lamp. The range of scanning was 400–750 nm with 1 nm increment.

Non-linear data fitting and PCA-SM calculations were performed using the MATLAB 4.0 software.

SERS experiments

SERS spectra were obtained for the molecules adsorbed on an electrochemically roughened silver electrode, which was prepared as follows. The electrode surface was polished mechanically to a mirror-like state. After this the electrode was washed with ethanol and triply distilled water, boiled in 0.1 M NaOH for 3 min, rinsed several times with triply distilled water and placed as a work electrode in a standard electrochemical cell filled with the 0.3 M KCl aqueous electrolyte solution. The second silver electrode and the platinum electrode were used as reference and auxiliary electrodes, respectively. An oxidation–reduction cycle was performed with a potentiostat-galvanostat IPC-4 (Institute of Physical Chemistry, Moscow, Russia) following the procedure optimized for a maximal enhancement of Raman signal: the electrode was maintained at the potential of −650 mV for 5 min, at 0 V for 60 s, at +250 mV for 15 s, at 0 V for 15 s and, finally, at −650 mV for 60 s. Roughened in this way the electrode was washed with triply distilled water, dried, and washed again with acetonitrile to remove electrolyte and water traces. For SERS measurements, the roughened electrode was immersed in the cell with the analyte solution. SERS spectra were recorded at an undefined electrode potential. The experiments were performed in the acetonitrile solution at a room temperature. Acetonitrile (HPLC grade) was doubly distilled from P_2O_5 and CaH_2 to remove water traces. As shown earlier,[14,15,20] the silver electrode is much more stable to organic solvents and high ion concentrations than other SERS-active substrates such as sols and metal island films. This unique property predefined the choice of silver electrode as a SERS-active substrate for the SERS study of **1a**,**b**,**c** in organic solvents.

SERS spectra were recorded with a Ramanor HG-2S spectrometer (Jobin Yvon, France) in the 900–1700 cm^{-1} range (1 cm^{-1} increment, 1 s integration time) and averaged over three scans. The spectral resolution of the spectrometer was 1 cm^{-1}. Excitation wavelengths (λ_{exc}) were 457.9 and 514.5 nm of an Ar-ion laser (Spectra-Physics, Model 164-03). The laser power was 50 mW. The computational procedure based on the Levenberg–Marquart method of curve fitting[27] was used to deconvolve the overlapped bands in SERS spectra and to determine the correct values of band intensities and

their maxima. No correction of the relative intensities of the bands for the device response was required in the spectral range (540–562 nm), where the SERS spectra were recorded.

SERS titration experiments ($\lambda_{exc} = 514.5$ nm) were performed for the compound **1b**, which was dissolved in acetonitrile (0.1 mM) and titrated with a stock solution of calcium perchlorate (0.2 M) supplemented with 0.1 mM of **1b**. This supplement was added to avoid a change in the concentration of **1b** during the titration with calcium perchlorate. Finally, the C_M/C_L molar ratios ranged from 0 to 100.

Contribution of the acetonitrile Raman bands to the SERS spectra of the studied compounds was very weak. The solvent spectrum was recorded under the same experimental conditions and subtracted from the SERS spectra after the careful normalization to the intensity of the 918 cm^{-1} band.

Methods of calculation

The semi-empirical computations were performed using the AMPAC 6.55 package.[28] The geometries of different conformations of merocyanines (TC and TT) and their complexed forms were fully optimised using the PM3 Hamiltonian[22] in the gas phase as well as in an aqueous medium. All geometries were completely optimised without symmetry constraint, *i.e.* at C_1 symmetry. The numerical self-consistent reaction field (SCRF) formalism has been extended to excited states as implemented in the semi-empirical package AMPAC[28] and employed to embrace the effect of the solvent.[25] To calculate the electronic spectra, the configurational interaction (CI) method was used. The active space includes twenty occupied and twenty unoccupied orbitals, all excitations were generated within this active space. Absorption ($S_0 \rightarrow S_1$) spectra and oscillator strengths were obtained by the CI method on the basis the PM3 optimised geometries in gas and solvent.

Acknowledgements

This work was supported by the INTAS (Grant 97-31193) and the Russian Foundation for Basic Research (Project 02-03-33058).

References

1 (*a*) J.-M. Lehn, *Supramolecular Chemistry. Concepts and Perspectives*, VCH, Weinheim, 1995, pp. 111–164; (*b*) A. P. de Silva, H. Q. N. Gunaratne, T. Gunnlaugsson, A. J. M. Huxley, C. P. McCoy, J. T. Rademacher and T. E. Rice, *Chem. Rev.*, 1997, **97**, 1515; (*c*) B. Valeur and I. Leray, *Coord. Chem. Rev.*, 2000, **205**, 3.
2 S. Shinkai, *Cation Binding by Macrocycles. Complexation of Cationic Species by Crown Ethers*, eds., Y. Inoue and G. W. Gokel, Marcel Dekker, Inc., New York, 1990, pp. 397–423.
3 S. P. Gromov and M. V. Alfimov, *Russ. Chem. Bull.*, 1997, **46**, 611.
4 H. Bouas-Laurent, A. Castellan, J.-P. Desvergne and R. Lapouyade, *Chem. Soc. Rev.*, 2001, **30**, 248.
5 O. Fedorova and S. Gromov, *Targets in Heterocyclic Systems. Chemistry and Properties*, ed., O. A. Attanasi and D. Spinelli, Societa Chemica Italina, Roma, 2001, 4, 205–229.
6 M. T. Stauffer, D. B. Knowles, C. Brennan, L. Funderburk, F.-T. Lin and S. G. Weber, *Chem. Commun.*, 1997, 287.
7 B. Van Germet, *Organic Photochromic and Thermochromic Compounds*, eds., J. C. Crano and R. Guglielmetti, Plenum Press, New York, 1999, pp. 112–140.
8 B. Van Germet and M. P. Bergomi, U.S. Pat. 5, 066,818, 1991.
9 E. N. Ushakov, S. P. Gromov, O. A. Fedorova, Y. V. Pershina, M. V. Alfimov, F. Barigelletti, L. Flamigni and V. Balzani, *J. Phys. Chem. A*, 1999, **103**, 11 188.
10 R. M. Izatt, K. Pawlak, J. S. Bradshaw and R. L. Bruening, *Chem. Rev.*, 1991, **91**, 1721.
11 J. Saltiel, D. F. Sears, J.-O. Choi, Y.-P. Sun and D. W. Eaker, *J. Phys. Chem.*, 1994, **98**, 35.
12 S. Nie and S. R. Emery, *Science*, 1997, **275**, 1102.
13 K. Kneipp, Y. Wang, H. Kneipp, L. T. Perelman, I. Itzkan, R. R. Dasari and M. S. Feld, *Phys. Rev. Lett.*, 1997, **78**, 1667.
14 O. A. Fedorova, Yu. P. Strokach, S. P. Gromov, A. V. Koshkin, T. M. Valova, M. V. Alfimov, A. V. Feofanov, I. S. Alaverdian, V. A. Lokshin, A. Samat, R. Guglielmetti, R. B. Girling, J. N. Moore and R. E. Hester, *New J. Chem.*, 2002, **9**, 1137.
15 (*a*) A. V. Feofanov, Yu. S. Alaverdian, S. P. Gromov, O. A. Fedorova and M. V. Alfimov, *J. Mol. Struct.*, 2001, **563–564**, 193; (*b*) M. Kerker, D. Wang and H. Chew, *Appl. Opt.*, 1980, **19**, 4159.
16 K. Fukuhara, K. Ikeda and H. Matsuura, *Spectrochim. Acta*, 1994, **50A**, 1619.
17 E. Vogel, A. Gbureck and W. Kiefer, *J. Mol. Struct.*, 2000, **550–551**, 177.
18 M. Kerker, D. Wang and H. Chew, *Appl. Opt.*, 1980, **19**, 4159.
19 V. M. Hallmark and A. Champion, *J. Chem. Phys.*, 1986, **84**, 2933.
20 A. Feofanov, A. Ianoul, V. Oleinikov, S. Gromov, O. Fedorova, M. Alfimov and I. Nabiev, *J. Phys. Chem. B*, 1997, **101**, 4077.
21 C. R. Cantor, P. R. Schimmel, *Biophysical chemistry*, Mir, Moscow, 1985, p.15.
22 J. J. P. Stewart, *J. Comput. Chem.*, 1989, **10**, 209.
23 U. Steiner, M. H. Abdel-Kader, P. Fischer and H. E. A. Kramer, *J. Am. Chem. Soc.*, 1978, **100**, 3190.
24 S. R. Marder, D. N. Beratan and L.-T. Cheng, *Science*, 1991, **252**, 103.
25 *Solvents and Solvent Effects in Organic Chemistry*, 2nd ed., VCH, Weinheim, 1988, p. 298.
26 L. Titze and T. Aicher, *Practical Organic Chemistry*, Mir, Moscow, 1999, pp. 420–421.
27 A. Feofanov, S. Sharonov, P. Valisa, E. Da Silva, I. Nabiev and M. Manfait, *Rev. Sci. Instrum.*, 1995, **66**, 3146.
28 M. J. S. Dewar, J. P. Stewart, J. M. Ruiz, D. Liotard, E. F. Healy and R. D. Dennington, II, *AMPAC version 6.55. Semichem.*, Shawnee, 1997–1999.